PERGAMON

International Journal of Heat and Mass Transfer 44 (2001) 4245–4256

International Journal of HEAT and MASS TRANSFER

www.elsevier.com/locate/ijhmt

Film condensation of water in a vertical tube with countercurrent vapour flow

S. Thumm, Ch. Philipp, U. Gross *

Institut für Wärmetechnik und Thermodynamik, Freiberg University of Technology, G.-Zeuner-Str. 7, D-09596 Freiberg, Germany

Received 18 May 2000; received in revised form 8 February 2001

Abstract

In this experimental investigation of condensation heat transfer, the effects of film Reynolds number Re_F, Prandtl number Pr_F and interfacial shear stress τ_V have been studied independently. For condensation without considerable interfacial shear stress τ_V, correlations from the literature are confirmed. In the case of increasing values of τ_V a reduction in heat transfer coefficients is found for $Re_F < 10$ and an increase for $20 < Re_F < 670$. With turbulent film the influence of the shear stress disappears. Apparently two opposite tendencies which balance each other are responsible for this: with low film Reynolds numbers, holding back the downward flow of liquid causes a deterioration of the heat transfer; with high Reynolds numbers, the intensification of waves and turbulent fluctuations causes an improvement. A correlation is suggested which predicts very well the influence of the vapour flow on the heat transfer as a function of τ_V and Re_F. For the friction factor of the two-phase flow, correlations from the literature can be confirmed.

Keywords: Condensation; Experiment; Heat transfer

1. Introduction

Heat transfer with film condensation in vertical pipes is influenced by the vapour flow usually occurring in practical applications. If vapour flows countercurrently to the liquid, the liquid is obstructed by the shear stress acting at the interface. Such conditions prevail in reflux condensers, in rectification systems, in open surface columns and particularly in gravitation heat pipes or thermosyphons.

An examination of the literature about ''heat transfer in film condensation'' shows that:

- For film condensation *without* shear stress at the interface and with *cocurrent* vapour flow numerous research works exist with considerable deviations from author to author.
- The predominant part of the experimental investigations of heat transfer with *countercurrent* vapour flow has been done with thermosyphons, where the following restrictions and problems normally occur:
  - no independent variation of vapour and film flow possible;
  - accumulation of inert gases in the condensation section;
  - usually only laminar film flow.
- The strong scatter of the experimental data (see [1,2]) points to a generally insufficient measuring accuracy. Neither are absolute values taken with sufficient accuracy nor do experimental values exist with high reproducibility which permits an accurate investigation of individual parameters like the vapour shear stress.
- Frequently only averaged heat transfer coefficients are reported. The few local values were often measured with heat flow sensors, whose accuracy is small.
- The friction factors for countercurrent two-phase flow are often based on investigations of cocurrent two-phase flow with very high shear stress or on flooding experiments.

In brief, the available experimental material is quantitatively as qualitatively insufficient for correlations

* Corresponding author. Tel.: +49-3731-392-684; fax: +49-3731-393-655.

E-mail address: gross@iwtt.tu-freiberg.de (U. Gross).

0017-9310/01/$ - see front matter
PII: S0017-9310(01)00067-9

Nomenclature

c_p	specific heat capacity
d	tube inner diameter
d_h	hydraulic diameter of the vapour cross-section, $d-2\delta$
E_{rel}	relative deviation
f	correction factor
$\mathscr{L}$	characteristic length, $(\nu_F^2/g)^{1/3}$
$\dot{m}_F$	film mass flow rate
N	exponent in Eq. (7)
Nu_F	local Nusselt number, $\alpha_F\mathscr{L}/\lambda_F$
Pr_F	Prandtl number, $\eta_F c_{p,F}/\lambda_F$
Re_F	film Reynolds number, $\dot{m}_F/(\pi d\eta_F)$
Re_V	vapour Reynolds number, $\bar{v}_V d_h/\nu_V$
$\bar{v}$	averaged velocity

Greek symbols

α	local heat transfer coefficient
δ	film thickness
δ^*	dimensionless film thickness, $\delta/\mathscr{L}$
η	dynamic viscosity
λ	thermal conductivity
ν	kinematic viscosity
ξ	friction factor
ρ	density
τ	shear stress
τ_V^*	dimensionless shear stress, Eq. (1)
τ_V^+	dimensionless shear stress, Eq. (2)
Ω	parameter, defined in Eq. (26)

Subscripts

calc	calculated
exp	experimental values
F	film
l	laminar
o	without vapour flow
t	turbulent
V	vapour
wavy	wavy film flow
δ	with influence of τ_V on film thickness

Superscripts

$*$	dimensionless variable, related to $\mathscr{L}$
$+$	dimensionless variable, related to δ
$\circ$	without condensation

concerning heat transfer. This requires further investigations with

- precise measurement of the *local* heat transfer coefficient;
- independent variation of vapour and liquid flow, i.e. no limitation on total condensation;
- minimization of the influence of inert gas at the position of the measurement;
- coverage of wide ranges for the main parameters (film Reynolds number Re_F, film Prandtl number Pr_F and interfacial shear stress τ_V).

2. Experimental investigation

2.1. Test rig

For the achievement of the objectives described in the preceding paragraph a test rig was built. It is schematically drawn in Fig. 1 and described in the following paragraphs. A more detailed description is given by Thumm [3].

2.1.1. Central vertical tube

The core of the test rig is a vertical tube 4.2 m in length with an inner diameter of 28.2 mm. Inside this tube, a film of saturated liquid flows downward and saturated vapour flows upward. The latter is caused to liquefy at the film surface in the condensation section (A2), where the tube is surrounded by an annular water-cooled gap. The cooling water can be fed into three different inlets of the condensation section, permitting three different lengths of the cooling zone (378, 828, 1621 mm). The local heat transfer coefficient is determined in the measuring section (A1) which is described in Section 2.1.4.

2.1.2. Vapour cycle

Saturated vapour produced in the evaporator (D1) flows upwards through the condensate separation device (A5) and the lower end of the vapour run-up section (A4). That part of the vapour flow which is not completely liquefied in the condensation section (A2) leaves the tube at the upper end and passes through the cyclone (Z1) for the separation of droplets which possibly have been entrained from the liquid film. The vapour is finally completely deposited in the condenser (W1) and led over the mass flow measurement device (F2 or F3) back to the evaporator (D1).

Pressure and saturation temperature in the system can be varied with the help of the condenser (W1). A PID controller adjusts the control valve R1 and thus the cooling water mass flow rate through the condenser. The cooling water itself is held at constant temperature by controlling the supply rate of cold water (R2).

2.1.3. Liquid cycle

From the overflow vessel of the condensate separation device (A5) an infinitely variable gear pump (P1) promotes a constant flow through the mass flow mea-

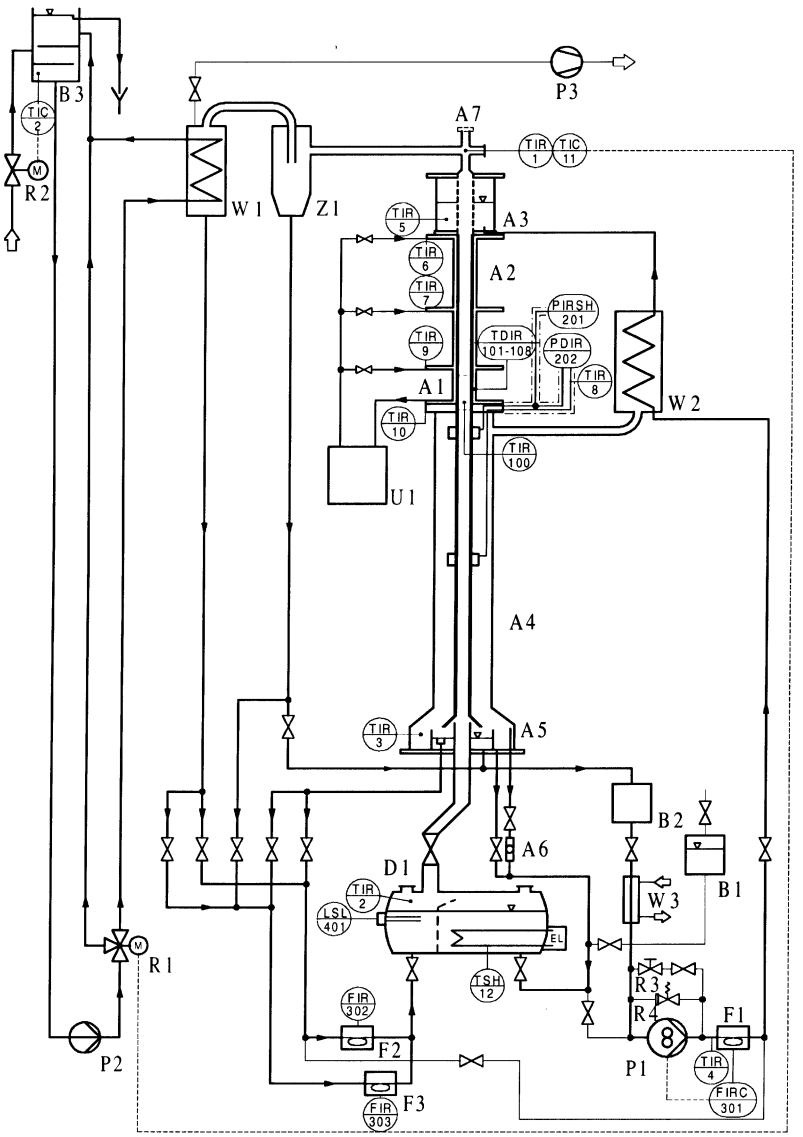

Fig. 1. Schematic drawing of the test rig. A1: measuring section; A2: condensation section; A3: film supply device; A4: vapour run-up section; A5: condensate separation device; A6: sight glass (level); A7: sight glass (condensation section); B1–3: storage vessels; D1: evaporator; F1–3: measuring of mass flow; P1: gear pump; P2: pump (cooling water); P3: vacuum pump; R1: control valve (condenser); R2: control valve (cooling water); R3: control valve (pump bypass); R4: relief valve; U1: circulation cooler; W1: condenser; W2: film heater; W3: cooler (liquid circuit); Z1: cyclone.

suring instrument (F1) to the film supply device (A3). Thereby the liquid is heated up to approximately saturation temperature in the film heater (W2). In the film supply device (A3) the liquid flows through a porous sinter tube to the inside of the main tube. In the condensation section (A2, A1) it is cooled and there it takes up additional liquid. In the condensate separation device (A5) the liquid film is separated from the countercurrent vapour flow and pours into the overflow vessel, where it is further separated with the help of the overflow into two streams: (a) that part which had been supplied in the device A3 will now start a new cycle and (b) the condensate which passes through the mass flow measuring device (F3 or F2) gets back into the evaporator.

In the film supply device (A3) almost saturated liquid is provided to the upper end of the condenser tube. Thus substantially higher film Reynolds numbers can be obtained than by exclusive condensation on the given condensation section. Additionally it enables a variation

of the film Reynolds number independent of the vapour flow.

2.1.4. Measuring section

The measuring section (see Fig. 2) consists of a thick-walled tube, into which thin thermocouples (diameter 0.5 mm) are brought directly underneath the inside and outside surfaces. With the measured radial temperature difference, the known thermal conductivity of the tube material and the known distance between the thermocouples the heat flux at the inner wall surface can be determined. With the measured temperature difference between inner tube wall and saturation temperature of the condensing vapour the local heat transfer coefficient can be calculated.

The calibrated thermocouples are inserted axially into the tube wall in blind-end bores with a length of 150 mm and with a diameter of 0.6 mm. The remaining gap is filled with tin solder. The drillings were brought in by spark erosion. In the capillary tube in the centre of the measuring section four thermocouples are inserted with a diameter of 0.25 mm each. Three of them are used for measuring the temperature difference between vapour and inner tube wall; one is used for the absolute measurement of the saturation temperature.

The measuring section was calibrated before the actual measurements. Therefore a heating coil was put inside the tube. The electric power of the coil as well as the temperature difference and the absolute temperature in the wall were measured and the thermal conductivity of the tube material (brass, $CuZn_{40}Mn_2$) was calculated. The result includes, and thus calibrates, the uncertainty of the position of the thermocouples inside the wall.

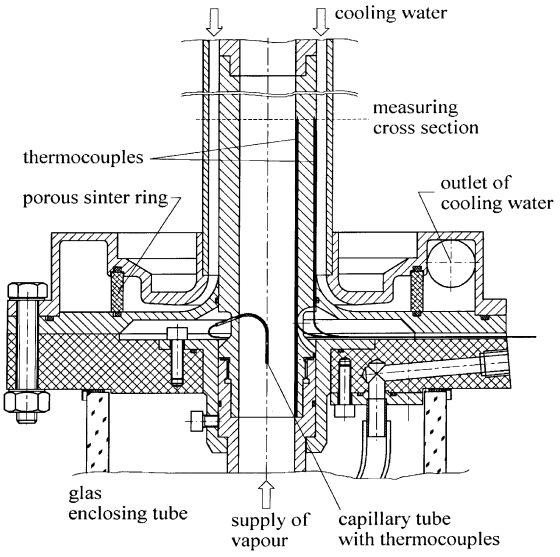

Fig. 2. Drawing of the measuring section.

2.2. Range of parameters

With the test rig described in Section 2.1, measurements were taken over wide parameter ranges:

- film Reynolds number: $1.3 < Re_F < 2100$;
- liquid Prandtl number: so far $2.5 < Pr_F < 4.3$, extension to $2.5 < Pr_F < 35$ is planned in the future;
- dimensionless shear stress at the liquid interface: $0 < \tau_V^* < 3.6$ and $0 < \tau_V^+ < 0.55$, respectively.

As additional parameters the temperature difference between saturated vapour and cooling water as well as the cooled length in the condensation section can be varied.

The shear stresses τ_V^* and τ_V^+ are characteristic parameters for the vapour–liquid interaction. They are defined as follows:

$$\tau_V^* = \frac{\tau_V}{g(\rho_F - \rho_V)\mathscr{L}}, \tag{1}$$

with the characteristic length $\mathscr{L}$ and the actual shear stress at the liquid interface τ_V. The dimensionless shear stress τ_V^+ contains instead of $\mathscr{L}$ the film thickness δ:

$$\tau_V^+ = \frac{\tau_V}{g(\rho_F - \rho_V)\delta}. \tag{2}$$

The shear stress τ_V can be calculated from well-known equations (see e.g. [4]) with the help of the friction factor ξ, which will be discussed in Section 3.4.

3. Representation and discussion of the results

A prerequisite for an accurate measurement of the local heat transfer coefficient is a completely developed flow and temperature profile in the measuring cross-section. In the case of supplying additional liquid at the top of the tube this is not necessarily true. By comparing measurements with different lengths of the cooling zone it could be proved that a cooling length of 828 mm, which is mostly used, produces no errors for $Re_F \leqslant 1010$. For the few measurements with higher Reynolds numbers the additional error is estimated as being smaller than 5%. This investigation is presented in detail by Thumm [3].

All measurements taken are presented in Fig. 3 in dimensionless form as the local Nusselt number Nu_F vs. the film Reynolds number Re_F. Ranges of the dimensionless shear stress τ_V^* are represented by various symbols. The experimental results are supplemented by the solution according to Nusselt's theory [5] and the predictions of Blangetti [6] (VDI-Wärmeatlas '94 [7]), Huhn [8], Mitrović [9] and Müller [10] (VDI-Wärmeatlas '97 [4]) as well as our own correlation. The curves in the diagram are valid for stagnant vapour. They can only be compared with the measurements having negligible interfacial shear ($\tau_V^* = 0$–0.3).

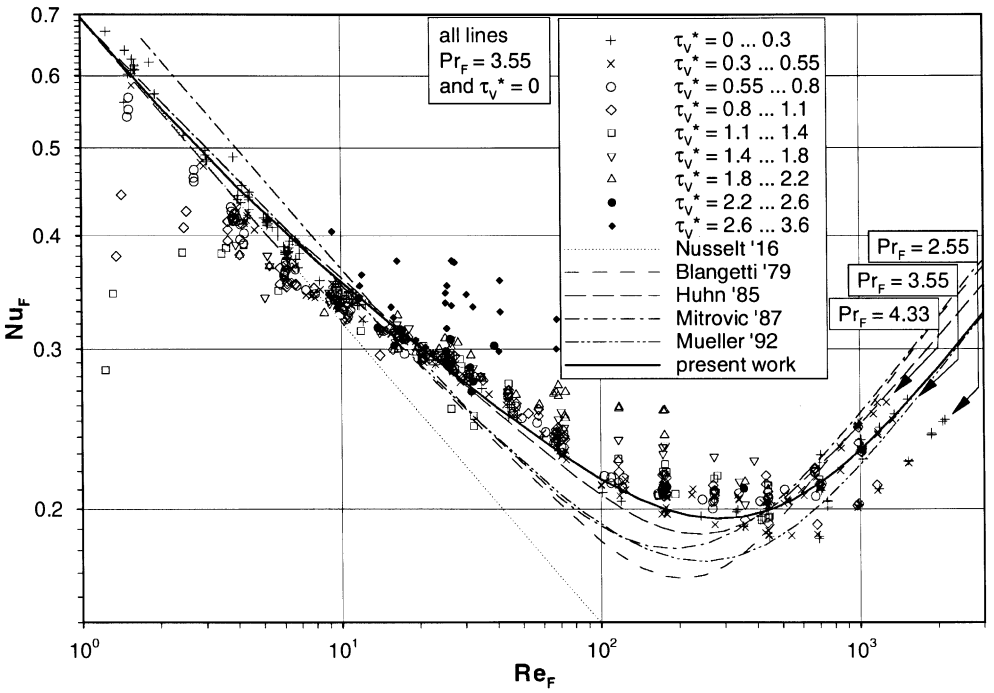

Fig. 3. Survey of measurements, present work.

3.1. Heat transfer with negligible interfacial shear

3.1.1. Superposition of laminar and turbulent Nusselt number

For a calculation of the heat transfer in the whole range of film flow a superposition of Nusselt number for laminar and turbulent flow is normally done in the following way:

$$Nu_F = \left(Nu_{F,l}^n + Nu_{F,t}^n\right)^{1/n}. \quad (3)$$

In the literature the exponent n varies between 2 and 4; our own measurements can be best correlated with $n = 2.5$.

As a consequence there is a gradual transition from the laminar curve to the turbulent curve as seen in the Nu_F, Re_F diagram in Fig. 3.

3.1.2. Laminar film flow

For the case of laminar wavy film flow the Nusselt solution corrected by the factor f_{wavy} (from Zazuli; see [11]) shows good agreement with our own measurements:

$$Nu_{F,l,o} = (3Re_F)^{-1/3} f_{wavy}, \quad (4)$$

with

$$f_{wavy} = 0.87 Re_F^{0.11} \quad \text{for } Re_F > 4. \quad (5)$$

A superposition of the equation for laminar film flow with that for turbulent film flow increases the calculated values in the transition region. In order to adjust this, the suggestion of Zazuli is somewhat amended by setting the exponent of the Reynolds number to 0.10.

In order to be able to calculate also Nusselt numbers with $Re_F < 4$ with one single equation, the equation for wavy film is combined with that for the smooth film in the following way:

$$f_{wavy} = \left[1^{20} + \left(0.87 Re_F^{0.1}\right)^{20}\right]^{0.05} = \left[1 + 0.062 Re_F^2\right]^{0.05}. \quad (6)$$

3.1.3. Turbulent film flow

Within the turbulent region of the film flow many suggestions exist which deviate considerably from each other especially with respect to the Prandtl number effect on heat transfer. In Fig. 4 the local Nusselt number is plotted vs. the liquid Prandtl number, including measurements by Müller [10], our own measurements and the results of some equations from the literature. All measured values are interpolated to the Reynolds number of $Re_F = 1000$. It can be seen that reliable measurements by Müller [10] with high Prandtl numbers up to $Pr_F = 50$ show substantially smaller Nusselt numbers than reported before. The measured values reported by Wassner [12] are too high in the laminar

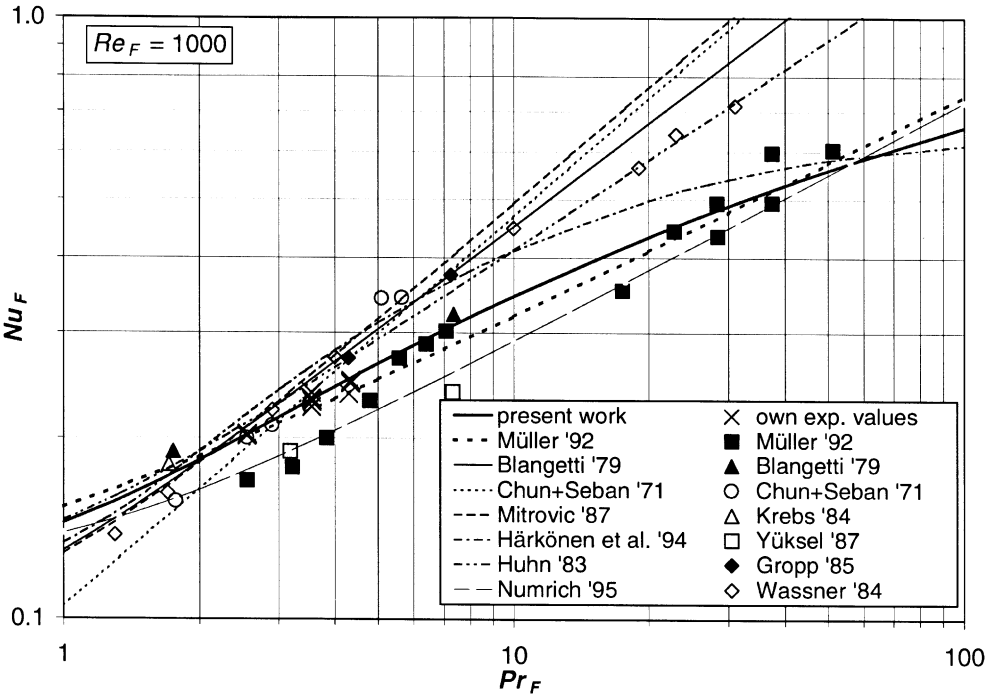

Fig. 4. Local Nusselt number as a function of the Prandtl number for $Re_F = 1000$, supplemented by additional experimental data from literature (see [10]).

region, so the values in Fig. 4 are probably too high as well.

In order to correlate our own measurements and at the same time the measurements by Müller [10], the exponent of the Prandtl number must depend on the Prandtl number itself. A similar method was suggested earlier by Härkönen [13]. The following relationship predicts our own measured values very well, but also those from Müller [10] with good agreement:

$$Nu_{F,t} = 0.007 Re_F^{0.38} Pr_F^N, \tag{7}$$

where

$$N = (1.3 + 0.24 \ln Pr_F)^{-1}. \tag{8}$$

3.2. Heat transfer affected by vapour flow

If the downward film flow is affected by a countercurrent vapour flow, the film is hampered from pouring down. The film thickness increases thereby with a tendency for the heat transfer to decrease. At the same time the shear stress at the film surface causes a reinforcement of the waves and the turbulence. This in turn leads to an improvement of the heat transfer. These two processes must be regarded separately from each other for both the laminar and turbulent film flow situation.

3.2.1. Enlargement of the film thickness

For *laminar* film flow the balance of momentum is solved with the vapour-side boundary condition of a shear stress at the interface in upward direction. An implicit equation for the dimensionless film thickness is obtained as a function of the film Reynolds number

$$Re_F = \frac{\delta_l^{*3}}{3} - \frac{\tau_V^*}{2}\delta_l^{*2}. \tag{9}$$

The film thickness can be calculated iteratively or by means of an approximation solution for the inverse function (9) which has been developed as:

$$\delta_l^* = 0.59\tau_V^* + (3^{1/3} - 0.0086\tau_V^*)(Re_F + 0.28\tau_V^{*3})^{1/3}. \tag{10}$$

This solution is valid for all τ_V^* occurring in countercurrent vapour flow with an error smaller than $\pm 1\%$.

The Nusselt number for laminar film conditions is then obtained from $Nu_F = \mathscr{L}/\delta = 1/\delta^*$:

$$Nu_{F,l,\delta} = [0.59\tau_V^* + (3^{1/3} - 0.0086\tau_V^*)(Re_F + 0.28\tau_V^{*3})^{1/3}]^{-1}. \tag{11}$$

This Nusselt equation should not be used on its own. It has to be combined with the correction factor for the reinforcement of turbulence which will be discussed in Section 3.2.2.

For *turbulent* film flow, Numrich [14] used a model for turbulent flow in a pipe and deduced a relationship between the film thickness with and without cocurrent vapour flow. This can be done in a similar way for countercurrent vapour flow:

$$\frac{\delta_t}{\delta_{t,o}} = \left(\frac{\delta_t}{\delta_{t,o}} - \tau^+_{V,o} \right)^{-1/2}. \tag{12}$$

Here $\tau^+_{V,o}$ is the dimensionless shear stress

$$\tau^+_{V,o} = \frac{\tau_V}{g(\rho_F - \rho_V)\delta_{t,o}}, \tag{13}$$

with the film thickness $\delta_{t,o}$, where the influence of the shear stress is not included. $\delta_{t,o}$ can be calculated with well-known equations from the literature, e.g. Eqs. (29) and (31).

Eq. (12) has to be evaluated iteratively, a procedure which can be avoided by the following approximation in the case of countercurrent vapour flow:

$$\frac{\delta_t}{\delta_{t,o}} = 1 + 0.43\tau^+_{V,o}. \tag{14}$$

By application of Eqs. (1) and (2) we get

$$\frac{\delta_t}{\delta_{t,o}} = 1 + 0.43\frac{\tau^*_V \mathscr{L}}{\delta_{t,o}} = 1 + 0.43\frac{\tau^*_V}{\delta^*_{t,o}}. \tag{15}$$

With an approach using the Reynolds analogy, Numrich [14] deduced a relationship between the turbulent Nusselt number with and without shear stress:

$$\frac{Nu_{F,t,\delta}}{Nu_{F,t,o}} = \frac{\delta_{t,o}}{\delta_t}. \tag{16}$$

Inserting Eq. (15) we get

$$\frac{Nu_{F,t}}{Nu_{F,t,o}} = (1 + 0.43\tau^+_{V,o})^{-1} = \left(1 + 0.43\frac{\tau^*_V}{\delta^*_{t,o}} \right)^{-1}. \tag{17}$$

Our own measurements for turbulent film flow have been analyzed and no influence of the vapour shear stress on the heat transfer could be found. Obviously the effects of thickening the film (degradation of heat transfer) and reinforcing the turbulence (improvement of heat transfer) are approximately balanced. Thus effectively no modification results. For this reason Eq. (17) is not used in our own work and we finally get

$$Nu_{F,t} = Nu_{F,t,o}. \tag{18}$$

3.2.2. Reinforcement of turbulence

In some theoretical investigations the reinforcement of turbulence is taken into account by a dependence of the eddy diffusivities on shear stress at the liquid interface (e.g. [6,9]).

Another model for the reinforcement of turbulence assumes that the resistance at the liquid interface approaches zero with very high vapour velocities. Claus [15] and Hadley [16] gave correction factors for laminar and turbulent flow. They tend towards a maximum value for very high vapour shear stresses. With moderate values these maximum correction factors are reduced as a function of the dimensionless shear stress τ^+_V.

These correction factors are given in the case of cocurrent condensation and for very high vapour shear stresses. In the case of countercurrent condensation comparatively small vapour velocities occur, since at higher values flooding first takes place and then cocurrent flow in an upward direction.

The suggested corrections [15,16] and the empirical ones from Lange [17] and Kellenbenz [18] reproduce our own measured values only very poorly. This becomes clear from Fig. 5, where the ratio between measured and calculated Nusselt numbers

$$\frac{Nu_{exp}}{Nu_{calc}} = f_\tau(\tau_V, Re_F) \tag{19}$$

is plotted vs. τ^+_V.

As can be seen, there exist systematic deviations depending on the film Reynolds number. Obviously the dimensionless shear stress τ^+_V, which is included in all of the suggested correction factors, does not describe the physical behaviour.

If the correction factor f_τ is plotted vs. τ^*_V, as in Fig. 6, only a very small effect of Re_F can be seen. The reinforcement of turbulence obviously depends directly on τ_V (as in τ^*_V) and not on τ_V/δ (as in τ^+_V).

For this reason a new empirical correction factor has been developed, which represents the present measurements much better than the existing correlations. It possesses the form

$$f_\tau = 1 + f_{\tau,\tau^*_V} f_{\tau,Re_F}, \tag{20}$$

whereby f_{τ,τ^*_V} and f_{τ,Re_F} represent the effects of τ^*_V and Re_F, respectively.

The dependency on τ^*_V results directly from a correlation of the data points in Fig. 6:

$$f_{\tau,\tau^*_V} = 0.12\tau^{*1.4}_V. \tag{21}$$

It is remarkable that measured values with $Re_F > 670$ are completely independent of the vapour shear stress. As already mentioned, the degradation of the heat transfer by increasing the thickness of the film and the improvement by the higher turbulence seem to neutralize each other in the case of turbulent film flow. For this reason corrections for the influence of the vapour flow are necessary only for laminar film flow.

The equations suggested so far are used for the prediction of the Nusselt number and are compared with our own measured values. They are then plotted vs. the film Reynolds number as shown in Fig. 7. Obviously there is a small dependency on Re_F which can be well correlated with the following equation:

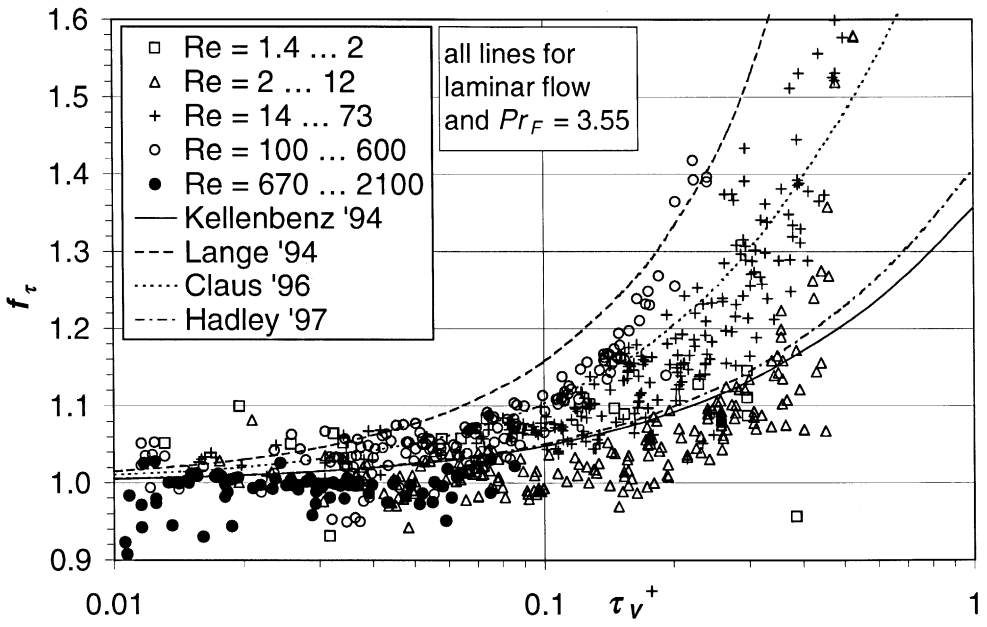

Fig. 5. Dependency of the reinforcement of turbulence on the dimensionless shear stress τ_V^+.

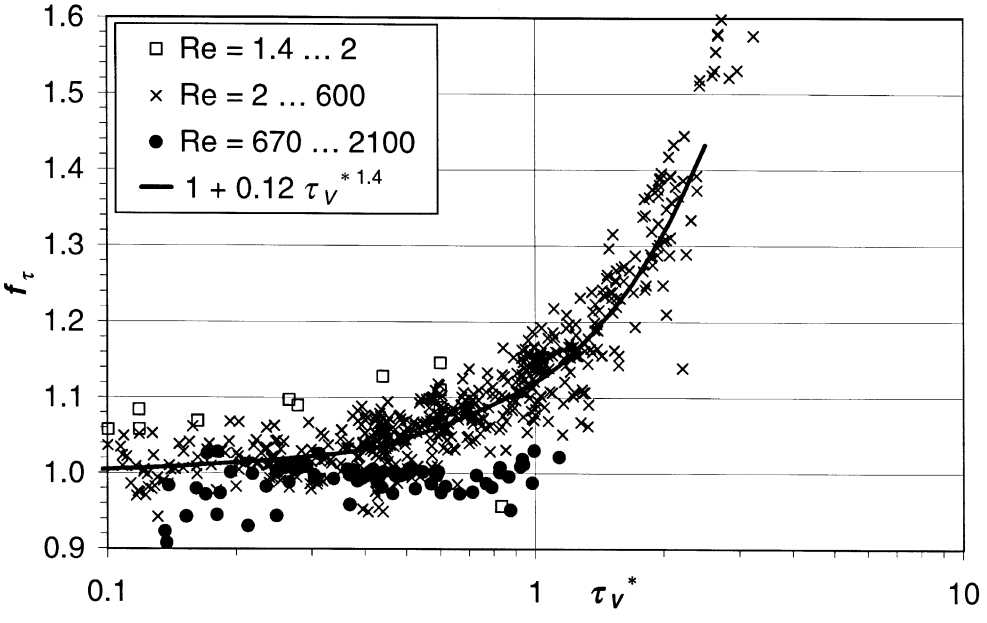

Fig. 6. Dependency of the reinforcement of turbulence on the dimensionless shear stress τ_V^*.

$$f_{\tau,Re_F} = 1.4 - \frac{0.65}{Re_F^{0.3}} - \frac{1.4}{1 + (2500 Pr_F^{-0.95}/Re_F)^4}. \quad (22)$$

Here the first term determines the maximum of the curve, the second term represents the reduction for low Reynolds numbers and the last term forces the steep decrease at $Re_F = 2500 Pr_F^{-0.95}$ to zero.

As a result, the following equation is suggested for the local heat transfer coefficient in the counterflow situation:

$$Nu_F = \left\{ [Nu_{F,l,\delta} f_{wavy}(1 + f_{\tau,\tau_V^*} f_{\tau,Re_F})]^{2.5} + Nu_{F,t}^{2.5} \right\}^{1/2.5}, \quad (23)$$

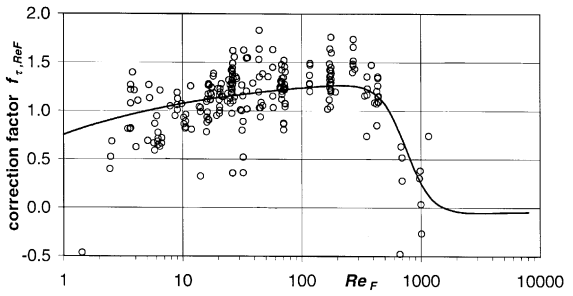

Fig. 7. Correction factor f_{τ,Re_F} as a function of the film Reynolds number.

whereby $Nu_{F,l,\delta}$ is calculated from Eq. (11), f_{wavy} from Eq. (6), f_{τ,τ_V^*} from Eq. (21), f_{τ,Re_F} from Eq. (22) and $Nu_{F,t}$ from Eq. (7).

In Fig. 8 our own measurements and the predictions of the suggested correlation are given for some values of τ_V^*. Clearly visible is the deterioration of heat transfer due to shear stress for $Re_F < 20$ and its improvement for $20 < Re_F < 1000$.

The deviation between correlated and measured values can be represented by

$$E_{rel} = \frac{Nu_{F,exp} - Nu_{F,calc}}{Nu_{F,exp}}, \tag{24}$$

as shown in Fig. 9. About 90% of all measured points can be correlated within a maximum deviation of ±5% and 99% within a maximum deviation of ±10%. Measurements with $\tau_V^* > 2.5$ are suspected to be in a flooding regime and thus are not considered.

3.3. Comparison of our own heat transfer correlation with measurements from the literature

The correlation compiled in this work is compared with experimental results from the literature. Measured values for local Nusselt numbers with countercurrent vapour flow and with independent mass flows, e.g. without complete condensation, are not found in the literature.

A comparison is only possible in the limiting case of $\tau_V \to 0$ (see Fig. 10). The values of Müller [10] are overpredicted, especially in the case of water. The values of Blangetti [6] and Krebs [19] for water agree quite well, but the systematic increase of the deviation with the Reynolds number indicates the problems they had with non-developed temperature profiles inside the liquid film.

In Fig. 11 the relative deviations between some other measurements from the literature and our own correlation are represented. The agreement with Struve [20] for high condensation lengths ($L = 1250$–800 mm like in our experiments) and with Wassner [12] for water is very

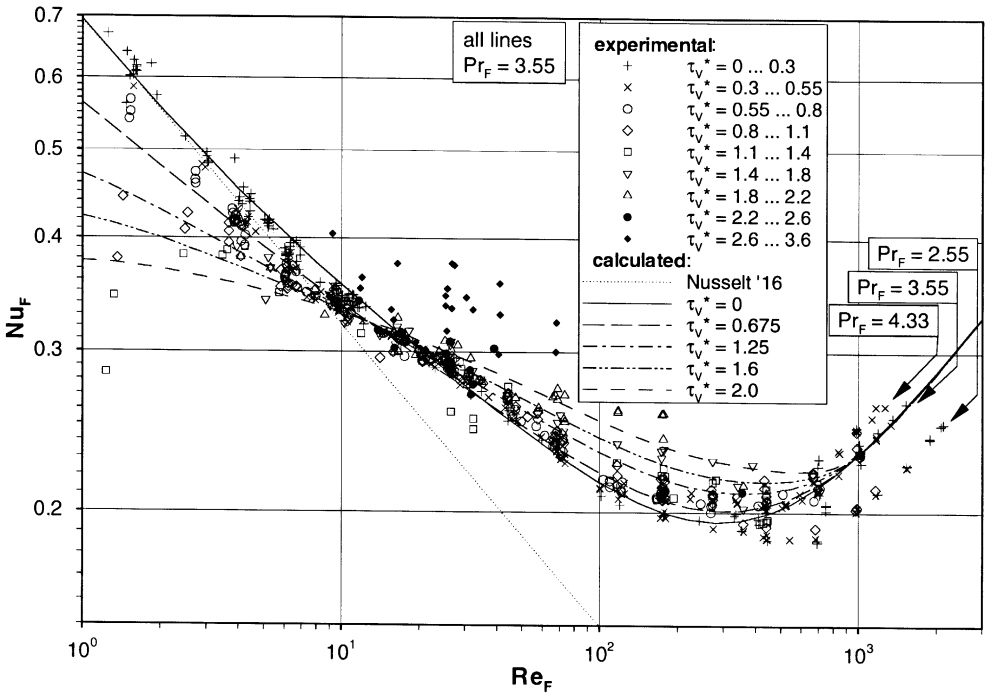

Fig. 8. Measurements and suggestion for some values of τ_V^*, drawn as the local Nusselt number vs. the film Reynolds number; present work.

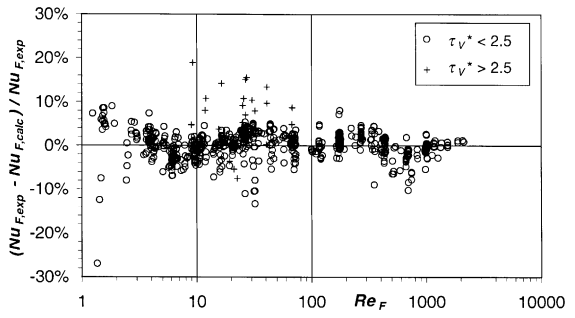

Fig. 9. Deviation between Eq. (23) and the present measurements.

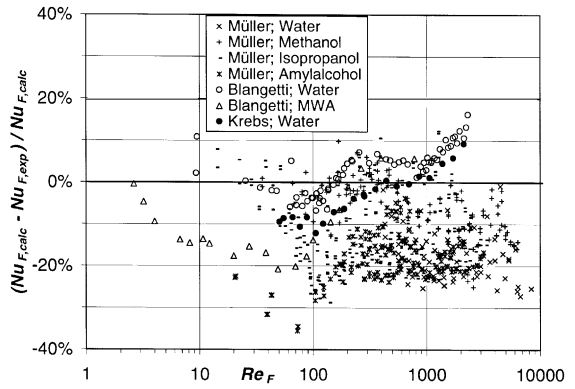

Fig. 10. Deviation between Eq. (23) and measurements from [6,10,19].

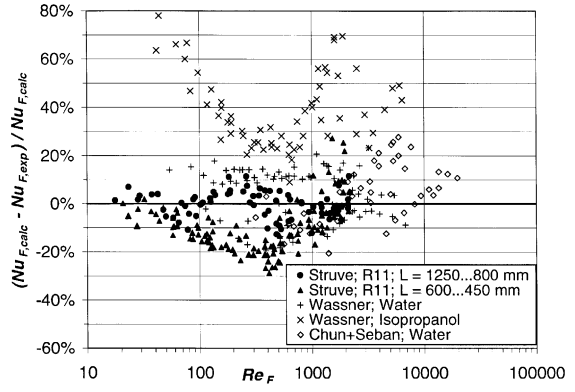

Fig. 11. Deviation between Eq. (23) and measurements from [11,12,20].

good. The values of Wassner [12] for isopropanol are strongly underpredicted even in the region of laminar film flow which is well covered by literature. Experiments of Chun and Seban [11] are quite well correlated with the new method.

3.4. Pressure drop and friction factor

The friction factor of the two-phase flow is calculated from measurements of the saturation temperature at two different locations: in the evaporator (TIR 2, see Fig. 1) and at the upper end of the central tube (TIR 1). With the temperature difference, the pressure drop can be calculated. Pressure drop in addition to the one for the two-phase flow is calculated and subtracted from the measurements. More details are communicated by Thumm [3]. The measured friction factor is compared with three correlations from the literature:

• In Brauer [21] a calculation procedure is suggested based on measurements of Feind [22] in the case of countercurrent flow of air/water and air/water–diethyleneglycol mixtures. These equations have been recommended by the VDI-Wärmeatlas '94 [7] and the friction factor can be calculated as

$$\zeta^{\circ} = \frac{358}{\Omega^2} + \frac{0.205}{\Omega^{0.25}}, \tag{25}$$

with

$$\Omega = c\frac{Re_V}{Re_F^n}\left(\frac{\rho_F}{\rho_V}\right)^{0.4}\left(\frac{\eta_V}{\eta_F}\right)^{0.67}\left(\frac{2\delta_o}{d}\right)^{0.5}. \tag{26}$$

The constants c and n are

$$c = 1.31, \quad n = 0.25 \qquad \text{for } Re_F < 40; \tag{27}$$

$$c = 4.76, \quad n = 0.60 \qquad \text{for } Re_F \geqslant 40. \tag{28}$$

The film thickness δ_o can be written in dimensionless form

$$\delta_o^* = \frac{\delta_o}{\mathscr{L}} \tag{29}$$

and δ_o^* can be calculated as:

$$\delta_{l,o}^* = (3Re_F)^{1/3} \qquad \text{for } Re_F \leqslant 513; \tag{30}$$

$$\delta_{t,o}^* = 0.303Re_F^{0.583} \qquad \text{for } Re_F > 513. \tag{31}$$

• Andreussi [23] modified an approach from [24]. The measurements were taken with cocurrent two-phase flow in an upwards direction, where high shear stress generally occurs. The calculation procedure is recommended by [4] also for the countercurrent flow situation.

• Hadley [16] modified the suggestion of Andreussi [23] slightly, in order to include two-phase flows with high gas densities in addition.

Fig. 12 shows the relative deviation of the calculated values (correlations by Brauer, Andreussi, Hadley) from our own measured values as a function of the *vapour* Reynolds number. Fig. 13 shows the relative deviation as a function of the *film* Reynolds number. No systematic effect can be detected with [21]. The influence of the

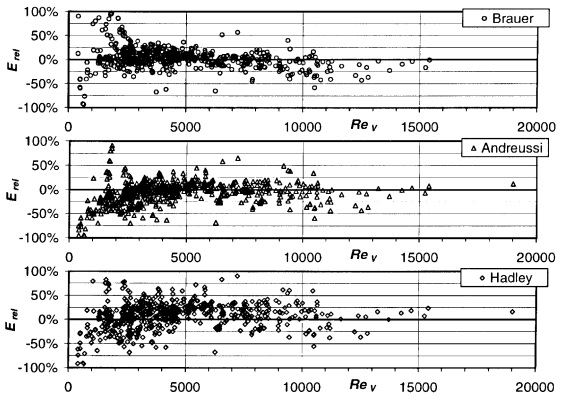

Fig. 12. Relative deviation of the calculated friction factor as a function of the vapour Reynolds number; $E_{\mathrm{rel}} = (\xi^{\circ}_{\mathrm{calc}} - \xi^{\circ}_{\mathrm{exp}})/\xi^{\circ}_{\mathrm{calc}}$.

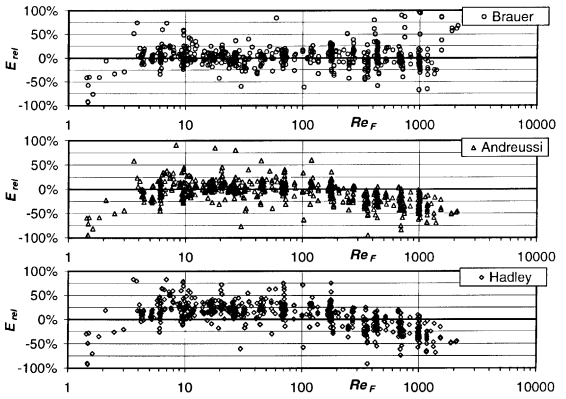

Fig. 13. Relative deviation of the calculated friction factor as a function of the film Reynolds number; $E_{\mathrm{rel}} = (\xi^{\circ}_{\mathrm{calc}} - \xi^{\circ}_{\mathrm{exp}})/\xi^{\circ}_{\mathrm{calc}}$.

film Reynolds number and thus the surface texture of the film is correctly correlated. The equations for the friction factors of Andreussi [23] and Hadley [16] tend to underpredict for high film Reynolds numbers.

The best results are obtained with the calculation of Brauer [21]. This was to be expected, since it is the only one based on measurements with countercurrent vapour flow.

4. Conclusions and final remarks

In this experimental study, condensation heat transfer inside a vertical tube has been investigated for the case of countercurrent flow of vapour (upwards) and liquid (downwards). Listed below are the major findings:

1. A test facility has been established which allows an independent variation of vapour and liquid mass flow rates, length of the cooling zone (in three steps) and heat flux.
2. Experiments are reported for pure water ($2.5 < Pr_{\mathrm{F}} < 4.3$) with the vapour and liquid Reynolds numbers within $0 < Re_{\mathrm{V}} < 15000$ and $1.3 < Re_{\mathrm{F}} < 2100$ respectively. This corresponds to dimensionless shear stresses of $0 < \tau^{*}_{\mathrm{V}} < 3.6$ and $0 < \tau^{+}_{\mathrm{V}} < 0.55$, with the upper limit given by the flooding effect.
3. In case of negligible interfacial shear and laminar film flow conditions, Nusselt's solution with the wave factor by Zazuli [11] shows good agreement with the experiments. For turbulent film flow, Müller's [10] results for the Prandtl number effect were confirmed and a new correlation is proposed with a variable exponent of the Prandtl number.
4. With increasing vapour flow and interfacial shear stress, two effects on heat transfer coefficients have been found: thickness of the film is increased and a reinforcement of turbulence is affected. These effects oppose each other with tendencies for a decrease and an increase of heat transfer, respectively. They seem to balance each other for the fully turbulent range ($Re_{\mathrm{F}} > 670$). In the transition range ($20 < Re_{\mathrm{F}} < 670$) a strong enhancement could be found, but a deterioration of heat transfer is present for $Re_{\mathrm{F}} < 10$, where the liquid film is too thin for establishment of turbulent structures.
5. A correlation is presented for the water results reported in this study, with 90% of all measured data being found within a deviation range of ±5%.

The reported experimental results for water are part of a more extensive work with additional fluids like ethanol and isopropanol. The respective data cover a much broader Prandtl number range and they will be presented later.

Acknowledgements

The support of this work by the Deutsche Forschungsgemeinschaft (DFG) is greatly appreciated.

References

[1] U. Gross, Kondensation und Verdampfung im geschlossenen Thermosyphon, VDI-Fortschritt-Berichte, Reihe 19, Nr. 46, VDI-Verlag, Düsseldorf, 1991.
[2] U. Gross, Reflux condensation heat transfer inside a closed thermosyphon, Int. J. Heat Mass Transfer 35 (2) (1992) 279–294.
[3] S. Thumm, Filmkondensation im senkrechten Rohr bei Gegenstrom von Dampf und Flüssigkeit, Dissertation, Technische Universität Bergakademie Freiberg, 2000.
[4] Verein Deutscher Ingenieure, VDI-Wärmeatlas: Berechnungsblätter für den Wärmeübergang, eighth ed., Springer, Berlin, 1997.
[5] W. Nusselt, Die oberflächenkondensation des wasserdampfes, VDI Z. 60 (27) (1916) 541–546 and 569–575.

[6] F. Blangetti, Lokaler Wärmeübergang bei der Kondensation mit überlagerter Konvektion im vertikalen Rohr, Dissertation, Universität Karlsruhe, 1979.
[7] Verein Deutscher Ingenieure, VDI-Wärmeatlas: Berechnungsblätter für den Wärmeübergang, seventh ed., VDI-Verlag, Düsseldorf, 1994.
[8] J. Huhn, Filmströmungen bei sich überlagernden einflüssen, Waerme- und Stoffuebertrag. 19 (2) (1985) 131–144.
[9] J. Mitrović, Wärmeübergang bei der Filmkondensation reiner gesättigter Dämpfe ansenkrechten Kühlflächen, VDI-Fortschritt-Berichte, Reihe 19, Nr. 22, VDI-Verlag, Düsseldorf, 1987.
[10] J. Müller, Wärmeübergang bei der Filmkondensation und seine Einordnung in Wärme- und Stoffübertragungsvorgänge bei Filmströmungen, VDI-Fortschritt-Berichte, Reihe 3, Nr. 270, VDI-Verlag, Düsseldorf, 1992.
[11] K. Chun, R. Seban, Heat transfer to evaporating liquid films, J. Heat Transfer 96 (1971) 391–396.
[12] L. Wassner, Wärmeübergangsmessungen für kondensation und verdampfung am lotrechten fallfilmverdampferapparat, Brennst.-Waerme-Kraft 36 (6) (1984) 258–266.
[13] M. Härkönen, et al., Heat transfer and hydrodynamics of falling liquid films, no. 115 in Acta Polytech. Scand. Mech. Eng. Ser., Finnish Academy of Technology, 1994.
[14] R. Numrich, Influence of gas flow on heat transfer in film condensation, Chem. Eng. Technol. 13 (1990) 136–143.
[15] N. Claus, Kondensation strömender reiner Dämpfe im senkrechten Rohr bei Drücken bis 15 bar, Dissertation, Universität Gesamthochschule Paderborn, 1996.
[16] M. Hadley, Kondensation binärer Dampfgemische unter dem Einfluß der vollturbulenten Gasströmung bei Drücken bis 13 bar, VDI-Fortschritt-Berichte, Reihe 3, Nr. 468, VDI-Verlag, Düsseldorf, 1997.
[17] J. Lange, Die partielle Kondensation zweier im flüssigen Zustand löslicher Komponenten aus einem Gas/Dampfgemisch im senkrechten Rohr bei erhöhtem Druck, Dissertation, Universität Gesamthochschule Paderborn, 1994.
[18] J. Kellenbenz, Wärmeübergang bei der Kondensation von strömenden Dämpfen reiner Stoffe und binärer Gemische, VDI-Fortschritt-Berichte, Reihe 3, Nr. 365, VDI-Verlag, Düsseldorf, 1994.
[19] R. Krebs, Kondensation von dampf in anwesenheit nichtkondensierbarer gase in turbulent durchströmten senkrechten kondensatorrohren, Fortsch. Ber. VDI-Z. 6 (153) (1984).
[20] H. Struve, Der wärmeübergang an einem verdampfenden rieselfilm, VDI-Forschungsh. (534) (1969).
[21] H. Brauer, Grundlagen der Zweiphasen- und Mehrphasenströmungen, Verlag Sauerländer, Aarau, 1971.
[22] K. Feind, Strömungsuntersuchungen bei Gegenstrom von Rieselfilmen und Gas in lotrechten Rohren, VDI-Forschungsh. 481, Beilage zu: Forschung auf dem Gebiete des Ingenieurwesens, Ausgabe B, Band 26, VDI-Verlag, Düsseldorf, 1960.
[23] P. Andreussi, The onset of droplet entrainment in annular downward flows, Can. J. Chem. Eng. 58 (8) (1980) 267–270.
[24] W. Henstock, T. Hanratty, The interfacial drag and the height of the wall layer in annular flows, AIChE J. 22 (6) (1976) 990–1000.